Transfer of Surface-Active Agents across a Liquid-Liquid Interface

DENNIS C. ENGLAND and JOHN C. BERG

University of Washington, Seattle, Washington

Analytical solutions are obtained for the transfer of an adsorbing solute across a liquid-liquid interface taking into account the effects of molecular diffusion in both bulk phases, adsorptive accumulation at the interface, and energy barriers to adsorption and/or desorption. These solutions show that while adsorptive accumulation alone affects the transfer rate but little, the presence of an adsorption or desorption barrier can significantly affect the bulk concentration profiles and decrease the mass transfer rate. The presence of a desorption barrier is shown to cause the dynamic interfacial tension to pass through a minimum below the steady state value. For some systems it is conceivable that the interfacial tension minimum would be sufficiently low that a slight agitation would result in spontaneous emulsification.

Dynamic interfacial tension data for oil-water systems with interface ages from 0.05 to 1.5 sec. are obtained using a laminar contracting liquid jet. The data indicate the presence of a small net desorption barrier to the transfer of normal and isobutyric acids from oil to water and large barriers to both the adsorption and desorption of 1,5 pentanediol.

The mass transfer of surface-active materials across a stagnant fluid interface may differ from the transfer of ordinary substances in at least two respects: (1) During the time period immediately following the formation of a fresh interface, the transient flux of solute into the receiving phase should be reduced due to adsorptive accumulation of solute at the interface. (2) The high degree of orientation of the solute molecules in the adsorbed state may lead to energy barriers to adsorption onto and/or desorption from the interface. Published adsorption, desorption, and mass transfer data provide ample, although often circumstantial, evidence of the importance of these effects. Barriers seem to be present at the air-water interface to the adsorption of certain molecules, such as those containing two hydrophillic groups separated from one another, for example, dibasic carboxylic acids (*6, 15*). Time effects in excess of those required for molecular diffusion have also been reported for adsorption at the liquid-liquid interface. Ward and Tordai (*32, 34* to *36*), using a pendant drop technique, reported diffusion coefficients backcalculated from the observed rate of interfacial tension lowering to be much less than conventional values for lauric, palmitic, and stearic acids; ethyl palmitate; and some aliphatic alcohols adsorbing from *n*-hexane onto its interface with water. It was found that a first-order adsorption reaction adequately described the process. Garner and Mina (*10, 11*), using a contracting jet, reported similar results for the adsorption of the C_3 to C_8 aliphatic acids, alcohols, and amines from water onto its interface against a medicinal paraffin oil.

Finally, there is a sizable literature on interfacial resistance to mass transfer. Considerable experimental evidence seems to indicate that transfer across the gas-liquid interface is free of resistance when foreign surfactant films are absent (*5, 6, 14, 22, 24*), although Chiang and Toor (*4*) and Baird and Davidson (*2*) have reported apparent small resistances. For transfer of surface-active materials across the liquid-liquid interface, however, many investigators have reported resistances of various magnitudes (*3, 10* to *12, 16* to *21, 23, 26, 27, 29* to *31, 37*). Using a laminar jet, Quinn and Jeannin (*21*) have reported an interfacial resistance of 80 sec./cm. to the transfer of isobutanol into water. Shimbashi and Shiba (*26, 27*), using a layer absorption technique, reported a resistance to the transfer of *n*-butyric acid from aqueous solution to CCl_4 and to benzene, and explained it in terms of a desorption activation barrier of 16 kcal./mole. Nitsch (*19, 20*), using rapidly formed drops, found that a second-order reaction rate expression described the transfer of several carboxylic acids from water to CCl_4 and that a half-order reaction described the transfer in the opposite direction. He explained this in terms of a dimerization or dissociation reaction in the interface. However, an adsorption or desorption barrier can be shown to yield the same rate dependence on concentration (*9*).

In some cases, involving the transfer of nonsurface-active materials, apparent interfacial resistances have been attributed to rather specific effects. Drickamer and coworkers, using a stagnant diffusion cell (*23, 28, 30*), reported large resistances (10^3 to 10^6 sec./cm.) associated with the transfer of sulfur across various liquid interfaces and attributed them to hydrogen bonding in the liquids. A time-independent interfacial resistance coefficient was used in their mathematical analysis. Duda and Vrentas (*8*) have generalized the analysis by employing a time-dependent coefficient. Lewis (*17*) and later McNamey (*18*) reported interfacial resistances associated with the transfer of inorganic nitrates from water to *n*-butanol and attributed them to the slow formation of a solvated complex at the interface.

For nonsurface-active or very slightly surface-active solutes, transfer rates in agreement with diffusion theory have often been found. Davies and Wiggill (*7*) studied the transfer of acetic acid and diethylamine between water and various oils, while Ward and Brooks (*33*) examined the transfer of acetic, propionic, *n*-butyric, and valeric acids across the water-toluene interface. Both investigations employed the direct determination of unsteady concentration profiles in unstirred diffusion cells, however, and were capable of detecting only resistances in excess of 1,000 sec./cm. Ward and Quinn (*37*), using the laminar jet technique mentioned earlier (*21*), detected no resist-

Dennis C. England is at Shell Development Corporation, Emeryville, California.

ance for the transfer of acetic acid and benzoic acid across the water-benzene interface, and possible (but small, < 20 sec./cm.) resistances associated with the transfer of oleic acid and cholesterol, both surface-active agents. The small resistances may have been the result of adsorptive accumulation.

The experimental methods employing the stagnant diffusion cell have the inherent disadvantage of being able to detect only very large interfacial resistances. Also, solute concentrations very near the interface cannot be determined accurately, and rather large contact times are required. Finally, such systems are often susceptible to interface contamination and interfacial turbulence. Various hydrodynamic arrangements that have been employed purport to decrease the detectable interfacial resistance to less than 20 sec./cm. and the contact time to as low as a few milliseconds. Great care must be taken, however, in accepting the results of studies in which there are highly complex or questionable hydrodynamic effects. Aside from the fundamental difficulty of describing the hydrodynamics, the flow studies reported thus far all have the disadvantage that the quantity measured experimentally is the integral amount of mass transfer, thus requiring indirect inference of the interfacial composition during the transfer process.

The question of the existence and importance of interfacial resistances to the transfer of solutes across a liquid-liquid interface must be regarded as unsettled. Aside from those specific cases in which the transfer processes are limited by slow chemical reaction at or near the interface, however, reports of interfacial resistance are very often associated with the transfer of surface-active solutes. Furthermore, barriers to adsorption and/or desorption, together with adsorptive accumulation, seem to provide a plausible qualitative explanation for these effects. Published analyses of interphase mass transfer data, however, have not taken these factors into account simultaneously. Finally, no experimental measurements of the time change of interfacial tension during unsteady mass transfer have been reported. Such measurements could provide a powerful means for detecting and following interfacial composition changes during mass transfer for the short contact times during which these effects would be expected to exert their greatest influence.

The purpose of the present study is thus twofold: First, it is desired to develop a sufficiently flexible theoretical model to describe the transfer of a surface-active agent across a liquid-liquid interface, taking into account the effects of adsorptive accumulation at the interface, bulk diffusion, and the presence of an activation barrier to adsorption and/or desorption. Second, it is desired to delineate these effects experimentally using the measurement of the time change of interfacial tension during mass transfer.

THEORY

Mass Transfer with Adsorptive Accumulation

The system to be considered consists of two semi-infinite immiscible bulk phases meeting at a plane interface, across which the solute is transferred. Initially phase 1 has uniform solute concentration x_0, while phase 2 is devoid of solute. The phases are brought together at time zero, and diffusive transfer ensues in accord with the equations (valid for dilute solution)

$$\frac{\partial x}{\partial t} = D_1 \frac{\partial^2 x}{\partial z_1^2}, \quad \text{in phase 1} \tag{1}$$

$$\frac{\partial y}{\partial t} = D_2 \frac{\partial^2 y}{\partial z_2^2}, \quad \text{in phase 2} \tag{2}$$

where x and y are solute concentrations in phases 1 and 2, respectively, and z_1 and z_2 are distances taken as positive moving away from the interface into phases 1 and 2, respectively. The initial conditions are

$$x = x_0 \text{ (for all } z_1), \quad y = 0 \text{ (for all } z_2), \quad \text{at} \quad t = 0 \tag{3}$$

and the boundary conditions

$$\frac{\partial x}{\partial z_1} = 0, \quad \frac{\partial y}{\partial z_2} = 0, \qquad z_1, z_2 = \infty \tag{4}$$

The two additional boundary conditions needed at the interface to specify completely the system are usually provided by a solute material balance (ignoring adsorption of solute):

$$D_1 \frac{\partial x}{\partial z_1} = -D_2 \frac{\partial y}{\partial z_2} \qquad z_1, z_2 = 0 \tag{5}$$

and an equation of solute distribution equilibrium (ignoring possible barriers to adsorption or desorption), such as

$$y = m\, x \qquad z_1, z_2 = 0 \tag{6}$$

If the effect of adsorption is to be taken into account, the mass balance (5) is inadequate and must be modified to require that the rate of transfer into a unit area of interface from phase 1 be equal to the rate of transfer out of a unit area into phase 2 plus the rate of accumulation in the interface:

$$D_1 \frac{\partial x}{\partial z_1} = -D_2 \frac{\partial y}{\partial z_2} + \frac{d\Gamma}{dt}, \qquad z_1, z_2 = 0 \tag{7}$$

where the amount adsorbed Γ has the units of mass per unit area. The equilibrium boundary condition (6) still applies as long as barriers are assumed absent. If the solutions are very dilute the amount adsorbed varies linearly with the bulk concentration in accord with

$$\Gamma = c\, x \tag{8}$$

where c is the adsorption equilibrium constant between the interface and phase 1.* With the additional stipulation that the amount adsorbed at time zero is zero, the following solutions may be obtained for the bulk phase concentration profiles and the amount adsorbed by the method of Laplace transforms:

$$x/x_0 = 1 - \beta \operatorname{erfc}\left(z_1/(2\sqrt{D_1 t}\right) - (1-\beta) \exp\left(-z_1^2/(4D_1 t)\right) e^{W_1^2} \operatorname{erfc}(W_1) \tag{9}$$

$$y/mx_0 = (1-\beta) \operatorname{erfc}\left(z_2/(2\sqrt{D_2 t}\right) - (1-\beta) \exp\left(-z_2^2/(4D_2 t)\right) e^{W_2^2} \operatorname{erfc}(W_2) \tag{10}$$

$$\Gamma/cx_0 = (1-\beta)\left[1 - \exp(\omega^2 t) \operatorname{erfc}(\omega\sqrt{t})\right] \tag{11}$$

where

$$\beta = m\left(m + \sqrt{\frac{D_1}{D_2}}\right)$$

$$W_i = \frac{m}{c\beta}\sqrt{D_2 t} + \frac{z_i}{2\sqrt{D_i t}}, \qquad i = 1 \text{ or } 2$$

and

$$\omega = (m/c\beta)\sqrt{D_2}$$

* c may be expressed as $c = \alpha/RT$, when $\alpha = -(\partial\sigma/\partial x)_{x=0}$ and σ is the interfacial tension. Values for α for a number of solutes at water-organic interfaces are presented in reference 25.

Figure 1 shows, in dimensionless coordinates, the effect of adsorptive accumulation on the concentration profiles near the interface a short time after contact. The dimensionless time depends on the diffusivity and on the adsorption coefficient c, so that $\theta = 1$ could correspond to a real time from 10^{-5} sec. (for butyric acid adsorbing from water to the water-air interface) to 0.1 sec. (for lauric acid adsorbing from water to its interface with n-hexane). In any case, the effect is confined to a region very near the interface (usually within 10^{-3} cm.). Figure 2 shows the adsorptive accumulation effect in terms of an apparent interfacial resistance to the transfer of solute across the interface for two representative examples. The interfacial resistance is defined as the total resistance to mass transfer in the presence of interfacial effects (in this case, adsorptive accumulation) minus the total resistance to transfer in the absence of these effects, that is

$$R_i = x_0/-D_2\left(\frac{\partial y}{\partial z_2}\right)^{\text{with ads}}_{z_2=0} - x_0/-D_2\left(\frac{\partial y}{\partial z_2}\right)^{\text{no ads}}_{z_2=0}$$

The value of the adsorption coefficient c yielding the upper curve of Figure 2 is typical for this parameter as encountered in practice; the value yielding the lower curve corresponds to some of the systems studied experimentally in the present work. The effect of interfacial accumulation, in terms of mass transfer resistance, is seen to be negligible for contact times in excess of a millisecond.

Mass Transfer in the Presence of Barriers

When there is resistance to mass transfer across the interface, the bulk concentrations adjacent to the interface may be far removed from distribution equilibrium so that a boundary condition alternate to Equation (6) must be developed. It is assumed here that the resistance may be attributed to first-order adsorption and/or desorption reactions as follows:

$$A_{\text{phase 1}} \underset{k_{-1}}{\overset{k_1}{\rightleftarrows}} A_{\text{adsorbed}} \underset{k_{-2}}{\overset{k_2}{\rightleftarrows}} A_{\text{phase 2}} \qquad z_1 = z_2 = 0$$

The net rate of adsorption from phase 1

$$\delta k_1 x - k_{-1}\Gamma, \qquad z_1 = 0$$

must be equal to the rate at which molecules enter a unit area of interface from phase 1, or

$$D_1\frac{\partial x}{\partial z_1} = \delta k_1 x - k_{-1}\Gamma, \qquad z_1 = 0 \qquad (12)$$

δ is the thickness of the adsorbed layer, introduced here to make the concentrations dimensionally consistent. Similarly the rate of desorption into phase 2 must equal the flux away from the interface in phase 2, or

$$k_2\Gamma - \delta k_{-2} y = -D_2\frac{\partial y}{\partial z_2}, \qquad z_2 = 0 \qquad (13)$$

1. Adsorption Barrier. The first case is obtained by considering the adsorption step to be slow, but the desorption into phase 2 to be essentially an equilibrium step. It may then be assumed that the amount adsorbed is related to the phase 2 subsurface concentration by

$$\Gamma = y\delta/K_{II} = \frac{c}{m}y, \qquad z_2 = 0 \qquad (14)$$

where $K_{II} = k_2/k_{-2}$ is the equilibrium constant. Equations (12) and (14) may be combined, making use of the relationship $K_I K_{II} = m$ to obtain the necessary boundary condition for the adsorption barrier case:

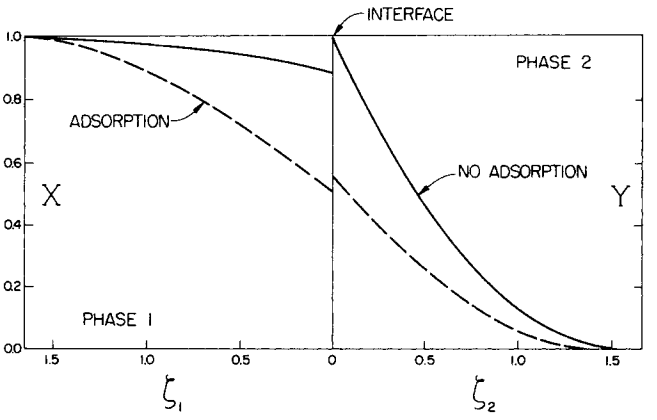

Fig. 1. The effect of adsorptive accumulation on the concentration profile for the case $\beta = 0.1$, $\theta = 1$.

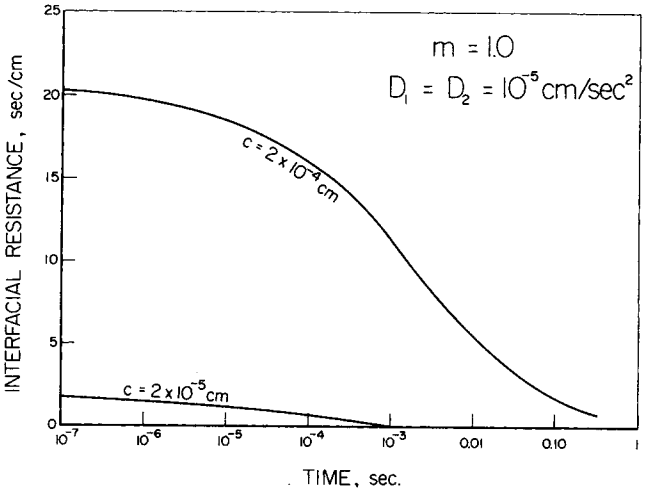

Fig. 2. Interfacial resistance due to adsorptive accumulation.

$$y = m\,x - \frac{m}{c}\frac{D_1}{k_{-1}}\frac{\partial x}{\partial z_1} \qquad z_I, z_2 = 0 \qquad (15)$$

Note that for an infinitely large rate constant this reduces to the equilibrium boundary condition (6).

Again, solutions are obtained by the method of Laplace transforms:

$$\frac{x}{x_0} = 1 - \beta\,\text{erfc}\,(z_1/(2\sqrt{D_1 t})) + \frac{\exp(-z_1^2/4D_1 t)}{(a-b)}\left[\left(\frac{c\,k_{-1}}{\sqrt{D_1}} - \beta b\right)e^{W_a{}^2}\,\text{erfc}\,(W_a) - \left(\frac{k_{-1}}{\sqrt{D_1}} - \beta a\right)e^{W_b{}^2}\,\text{erfc}\,(W_b)\right] \qquad (16)$$

$$\frac{y}{mx_0} = (1-\beta)\left\{\text{erfc}\,(z_2/(2\sqrt{D_2 t})) + \frac{\exp(-z_2^2/(4D_2 t))}{(a-b)}\left[b\,e^{W_a{}^2}\,\text{erfc}\,(W_a) - a\,e^{W_b{}^2}\,\text{erfc}\,(W_b)\right]\right\} \qquad (17)$$

$$\Gamma/cx_0 = (1-\beta)\left[1 + b\,e^{a^2 t}\,\text{erfc}\,(a\sqrt{t}) - a\,e^{b^2 t}\,\text{erfc}\,(b\sqrt{t})/(a-b)\right] \qquad (18)$$

where

$$a = \frac{1}{2}\left(\eta + \sqrt{\eta^2 - 4k_{-1}/(1-\beta)}\right)$$

$$b = \frac{1}{2}\left(\eta - \sqrt{\eta^2 - 4k_{-1}/(1-\beta)}\right)$$

$$\eta = c\frac{k_{-1}}{\sqrt{D_1}} + \frac{m}{c}\sqrt{D_2}$$

$$W_a = a\sqrt{t} + z_i/(2\sqrt{D_i t}),\ W_b = b\sqrt{t} + z_i/(2\sqrt{D_i t});\quad i = 1, 2$$

In general, a and b are complex.

2. *Desorption Barrier.* A second case is obtained by considering the adsorption step to be rapid, but the desorption into phase 2 to be limited. The amount adsorbed can once again be related to the phase 1 subsurface concentration by the linear relationship

$$\Gamma = K_1\delta x = cx \qquad z_1 = 0 \tag{19}$$

Equations (13) and (19) are combined to obtain the necessary boundary condition for the desorption barrier case:

$$y = mx + \frac{m}{c}\frac{D_2}{k_2}\frac{\partial y}{\partial z_2} \qquad z_1, z_2 = 0 \tag{20}$$

Again, this reduces to the equilibrium boundary condition for an infinitely large rate constant.

The solutions obtained for this case are

$$\frac{x}{x_0} = 1 - \beta\,\mathrm{erfc}\left(z_1/(2\sqrt{D_1 t})\right) - \frac{\exp(-z_1^2/(4D_1 t))}{(a-b)}\left\{\left[\left(\frac{\sqrt{D_1}}{c} - (1-\beta)b\right)\right] e^{W_a^2}\,\mathrm{erfc}\,(W_a) - \left[\left(\frac{\sqrt{D_1}}{c} - (1-\beta)a\right)\right] e^{W_b^2}\,\mathrm{erfc}\,(W_b)\right\} \tag{21}$$

$$\frac{y}{mx_0} = (1-\beta)\left\{\mathrm{erfc}\left(z_2/(2\sqrt{D_2 t})\right) + \frac{\exp(-z_2^2/(4D_2 t))}{(a-b)}\left[b\,e^{W_a^2}\,\mathrm{erfc}\,(W_a) - a\,e^{W_b^2}\,\mathrm{erfc}\,(W_b)\right]\right\} \tag{22}$$

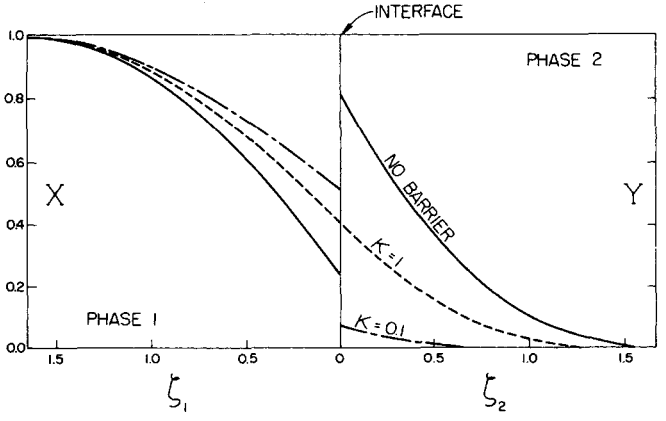

Fig. 3. The effect of a desorption barrier on the concentration profile for the case $\beta = 0.7$, $\theta = 1$.

$$\frac{\Gamma}{cx_0} = (1-\beta)\left[1 + \left(b^{a^2 t}\,\mathrm{erfc}\,(a\sqrt{t}) - a\,e^{b^2 t}\,\mathrm{erfc}\,(b\sqrt{t})\right)/(a-b)\right] - \frac{\sqrt{D_1}}{c}\left(e^{a^2 t}\,\mathrm{erfc}\,(a\sqrt{t}) - e^{b^2 t}\,\mathrm{erfc}\,(b\sqrt{b})\right)/(a-b) \tag{23}$$

where

$$a = \frac{1}{2}\left(\eta + \sqrt{\eta^2 - 4k_2/\beta}\right)$$

$$b = \frac{1}{2}\left(\eta - \sqrt{\eta^2 - 4k_2/\beta}\right)$$

$$\eta = \frac{c}{\sqrt{D_2}}\frac{k_2}{\beta}(1-\beta) + \frac{\sqrt{D_1}}{c}$$

and W_a and W_b are defined as in the adsorption barrier case.

3. *Adsorption and Desorption Barriers Simultaneously Present.* In this case the rate of adsorption from phase 1 and the rate of desorption into phase 2 are given by Equations (12) and (13), which may be combined to eliminate Γ and give the boundary condition

$$y = m\,x + \frac{m}{c}\left[\frac{D_2}{k_2}\frac{\partial y}{\partial z_2} - \frac{D_1}{k_{-1}}\frac{\partial x}{\partial z_1}\right] \tag{24}$$

Equation (13) may then be combined with the mass balance boundary condition (7) to eliminate Γ from that boundary condition. The concentration profiles can be obtained after application of Laplace transforms and much algebra. However, only the amount adsorbed is presented here:

$$\frac{\Gamma}{cx_0} = a(1-\beta)\left\{\frac{1}{(r_1-r_2)(r_1-r_3)r_1}\left[1 + (br_1 - 1)e^{r_1^2\theta}\,\mathrm{erfc}\,(r_1\sqrt{\theta})\right] + \frac{1}{(r_1-r_2)(r_3-r_2)r_2}\left[1 + (br_2 - 1)e^{r_2^2\theta}\,\mathrm{erfc}\,(r_2\sqrt{\theta})\right] - \frac{1}{(r_1-r_3)(r_3-r_2)r_3}\left[1 + (br_3 - 1)e^{r_3^2\theta}\,\mathrm{erfc}\,(r_3\sqrt{\theta})\right]\right\} \tag{25}$$

where

$$a = \frac{c^4 k_{-1} k_2}{8D_1^2\beta}$$

$$b = \frac{2\beta D_1}{\sqrt{\pi}\,c^2(1-\beta)k_2} \tag{26}$$

$$\theta = \frac{4}{\pi}\frac{D_1}{c^2}t$$

and r_1, r_2, and r_3 are roots of the cubic equation

$$a + d\phi + e\phi^2 + \phi^3 = 0$$

and

$$d = \frac{\pi}{4}\left[\frac{c^2}{D_i}(k_{1-} + k_2) + \frac{c^4}{D_1}k_{-1}k_2\frac{(1-\beta)}{\beta}\right]$$

$$e = \frac{\sqrt{\pi}}{2}\frac{c^2}{D_1}\left[k_{-1} + \frac{(1-\beta)}{\beta}k_2\right]$$

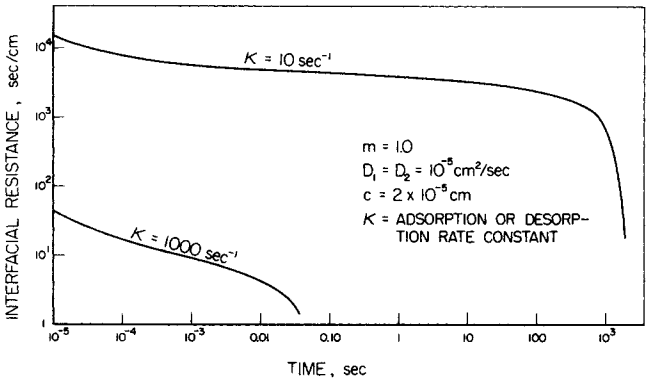

Fig. 4. Interfacial resistance due to adsorption or desorption kinetics.

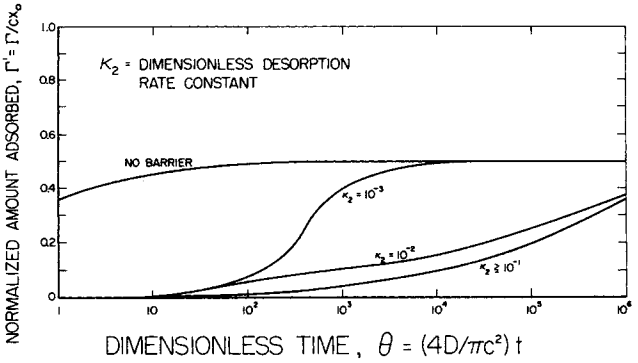

Fig. 6. Time dependence of the amount adsorbed in the presence of both adsorption and desorption barriers; $\beta = 0.5$, $\kappa_1 = 10^{-3}$.

All of the above equations may be made dimensionless by the introduction of the following dimensionless variables:

$$\text{Rate constant:} \quad \kappa_1 = c^2 \frac{k_{-1}}{D_1}, \quad \kappa_2 = c^2 \frac{k_2}{D_1} \qquad (27)$$

Time: defined in Equation (26) above

Distance from the interface: $\zeta_1 = z_1/(c\sqrt{\pi}), \quad \zeta_2 = z_2 \dfrac{\sqrt{(D_1/D_2)}}{c\sqrt{\pi}}$

$$\text{Concentration:} \quad X = \frac{x}{x_0}, \quad Y = \frac{y}{mx_0(1-\beta)}$$

After the appropriate substitutions the equations are found to depend only upon the parameters K_1, K_2, and β and the variables ζ_1, ζ_2, and θ.

The effect of desorption barriers on the concentration profiles, in dimensionless coordinates, is shown in Figure 3, while the effect of barriers to adsorption or desorption is shown in terms of interfacial resistance for two representative examples in Figure 4. Depending upon the magnitude of the rate constant for adsorption or desorption, the interfacial resistance may be large and remain large for long periods of time. The effect of adsorption or desorption barriers is shown in terms of the amount of adsorption in Figures 5 to 7. The most interesting curves are those for the amount adsorbed in the presence of a desorption barrier alone. In this case the supply of solute to the interface from phase 1 may be much greater than the desorption into phase 2, so that, as shown in Figure 5, the amount adsorbed rises to a maximum and then falls to the steady state value. The maximum interfacial concentration would be attained in the case of an infinitely high desorption barrier for which the amount adsorbed would reach equilibrium with the initial phase 1 concentration x_0. For intermediate desorption barriers, the interfacial concentration will rise to some value between the steady state and the maximum until the concentration driving force for desorption into phase 2 becomes greater than that for diffusion to the interface from phase 1. Then the amount adsorbed begins to drop and eventually approaches the steady state value.

The interfacial tension, corresponding to the maximum in the amount adsorbed, passes through a minimum, which for a given initial concentration, as shown in Figure 8, depends on the magnitude of the rate constant; the smaller the rate constant the lower the minimum and the longer the time required to reach the minimum. It is conceivable that under the right conditions this minimum in the dynamic interfacial tension could be low enough such that a slight agitation would result in so-called spontaneous emulsification.

The behavior of the amount adsorbed in the presence of both an adsorption and a desorption barrier is shown in Figures 6 and 7. It can be seen that for one of the dimensionless rate constants two or more orders of magnitude greater than the other, the adsorption curve approaches that of a single barrier corresponding to the smaller rate constant.

Extension of all the above analyses to include the more general case of nonlinear equilibrium adsorption is presently being undertaken.

EXPERIMENT

The interesting predicted behavior of the interfacial tension made it desirable to design an experiment such that the dynamic interfacial tension could be measured during interfacial mass transfer at short contact times. One method that has been used in the past with reasonable success for measuring the dynamic interfacial tension at a liquid-liquid interface is that of the laminar contracting jet (*1, 10* to *12*). The method is relatively

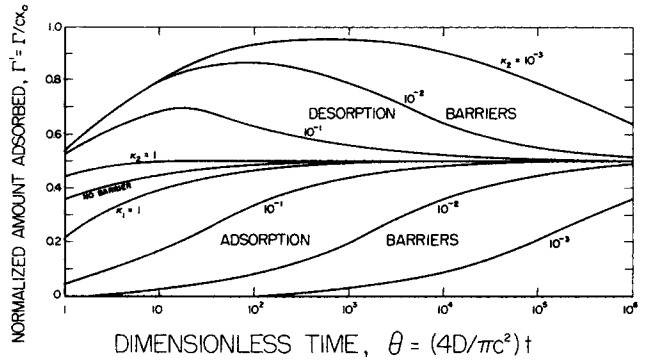

Fig. 5. Time dependence of the amount adsorbed in the presence of either an adsorption or desorption barrier for case $\beta = 0.5$.

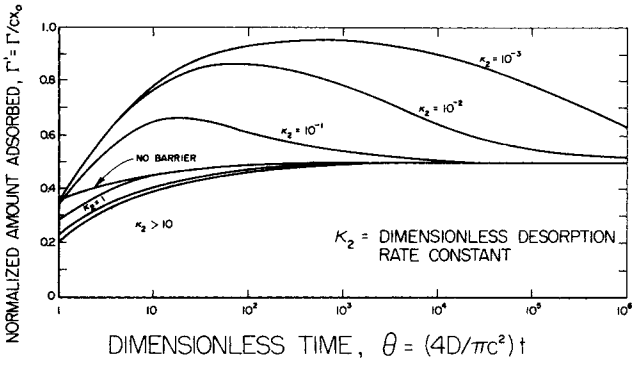

Fig. 7. Time dependence of the amount adsorbed in the presence of both adsorption and desorption barriers; $\beta = 0.5$, $\kappa = 1$.

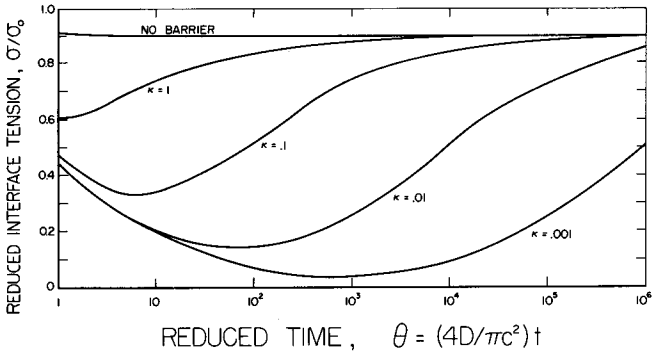

Fig. 8. Time dependence of the interfacial tension in the presence of a desorption barrier. The initial concentration, $x_0 = \sigma_0/(\partial\sigma/\partial x)_{x\to 0}$ and $\beta = 0.9$.

simple and may be used for contact times of a few hundredths of a second up to about a second.

When a liquid issues downward from a circular nozzle or orifice, it accelerates, causing the jet to contract. The interfacial tension acts to counteract this contraction: the greater the interfacial tension the less the contraction. An approximate energy balance may be written for the jet assuming potential flow

$$\frac{Q^2}{2\pi^2 r^4} + \frac{\sigma}{\rho_w}(1/R_1 + R_2) - g\,h\,(1 - \rho_o/\rho_w) = \text{constant} \tag{30}$$

Over most of the jet length, $(1/R_1 + 1/R_2)$ is well approximated by $1/R$.

Garner and Mina (*10*) have shown that for given flow rate, phase densities, and nozzle diameter, the interfacial tension can be well correlated with r and h only along much of the jet length. A nozzle can then be calibrated for a given flow rate using pure outer phase liquids of the same density but different interfacial tension against the pure jet liquid. It is assumed in applying the calibration data to a jet in which the interfacial tension varies along its length that this same relationship among σ, r, and h applies.

It remains then to determine the age of the interface as a function of distance from the nozzle. It is assumed in this analysis that an element of interface is created at the nozzle and moves down the jet at the interfacial velocity. If the velocity of the interface can be determined, the age at a distance h from the nozzle can be determined by numerical integration of $t = \int_0^h 1/u_{if}\,dh'$ where u_{if} is the interfacial velocity.

The velocity of the interface was determined by photographing with a motion picture camera tiny flakes of aluminum moving along the interface. The aluminum flakes in a dilute oil suspension were very slowly injected above the nozzle into the oil phase, using a Sage variable-speed syringe pump, through a 22-gauge syringe needle bent 90 deg. so that the flow out was horizontal. The jet was lighted from the side with a strobe light synchronized with the shutter of the camera; the particles moved too fast for conventional lighting. A small mirror was placed on the side opposite the strobe light to provide more nearly even illumination. Following Garner and Mina (*11*), distance against time curves for a large number of particles at various flow rates were obtained, permitting the unambiguous determination of interfacial velocity.

Apparatus and Procedure

The jet chamber was constructed of aluminum with plate glass windows sealed with Teflon gaskets. The nozzle and receiver were brass. The nozzle was tapered to a sharp edge and had an outer diameter of 0.8 cm. Figure 9 is a schematic diagram of the flow system. The tubing above the nozzle was of polyethylene or glass except for short connecting pieces of Tygon.

In making a run the chamber was first filled to the tip of the overflow tube *I* with the oil phase. Then the water flow was started from the supply tank *A*. Valves *F* and *K* upstream from

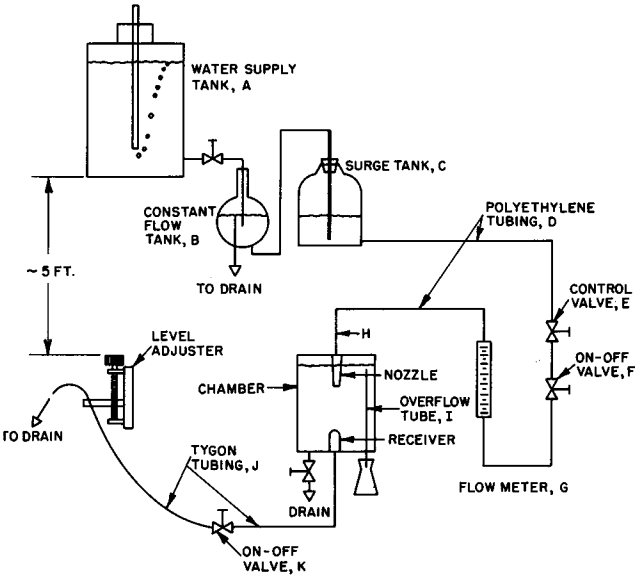

Fig. 9. Diagram of flow system.

the nozzle and downstream from the receiver were simultaneously opened, the jet flow rate was adjusted with control valve *E*, and the exit level *L* was adjusted so that the flow out equalled the flow of the jet.

The jet was backlighted with a 150-w. flood light. A copper sulfate solution was placed between the light source and the chamber to absorb the heat. A sheet of aluminum with a 0.50-in. wide vertical slit was also placed in front of the light to reduce further the amount of heat reaching the chamber and to provide a beam of light just wide enough to illuminate the

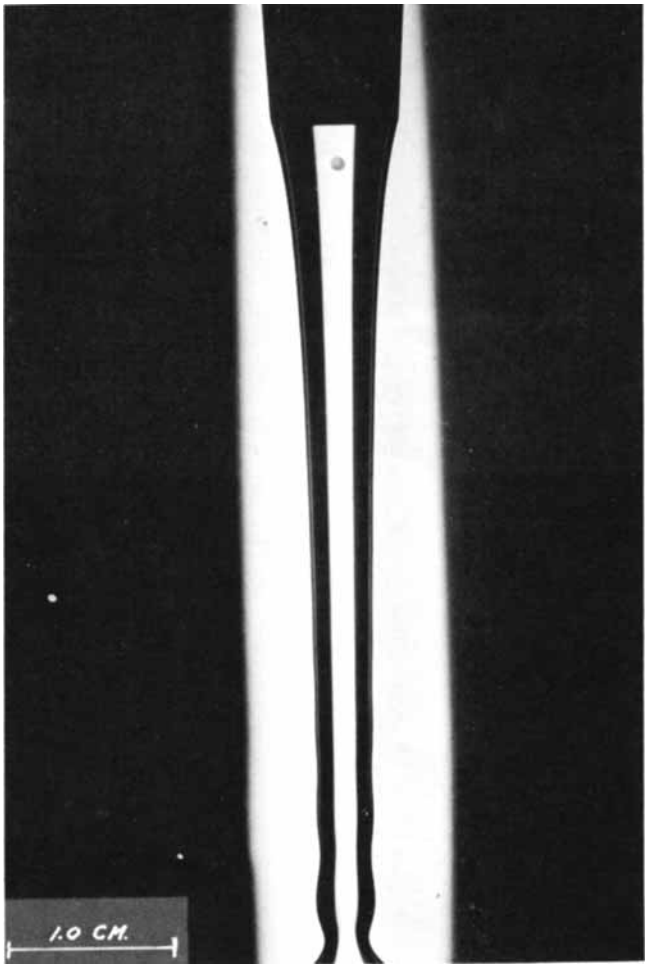

Fig. 10. Photograph of contracting jet.

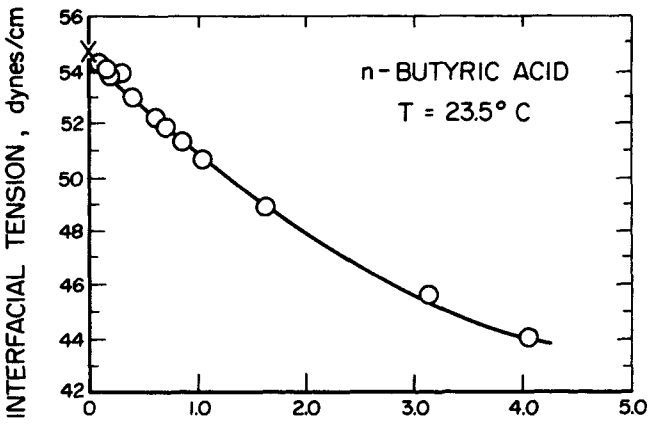

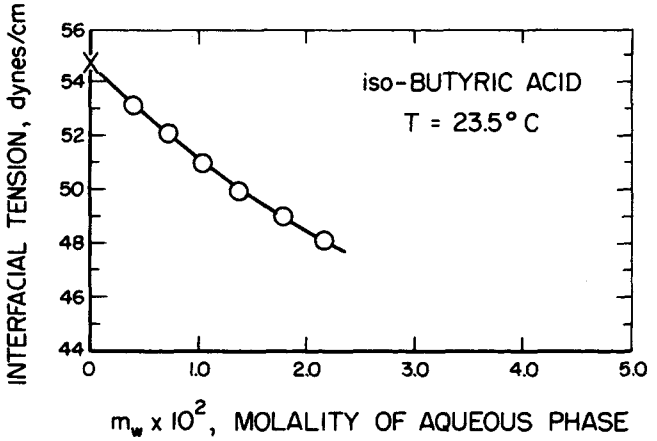

Fig. 11. Adsorption isotherms for *n*-butyric and isobutyric acids at the water-Marcol 70 interface.

jet. The jet, as shown in Figure 10, was photographed with a 4X5 Kodak Masterview camera using Panatomic-X film.

The jet dimensions were determined on a Vanguard Motion Analyzer capable of measurements to 0.001 in. on the magnified picture. The image was magnified 1.7 times on the negative and further magnified 16 times on the motion analyzer. Total magnification was about 27 times.

Systems Studied

Distilled water was used as the jet liquid. It was found, after several organic liquids were tried as the chamber liquid, that the outer liquid must be quite viscous in order to obtain a stable jet at the flow rates of interest. Marcol-70 white oil with a viscosity of 22 centipoise and density of 0.8573 g./cc. at room temperature was chosen. The interfacial tension of the pure oil against water is 54.7 dynes/cm.

The solutes studied were *n*- and isobutyric acids and 1,5-pentanediol. These are soluble in both phases, although they favor the water phase. The dynamic interfacial tension was studied for both transfer from water to oil and from oil to water. Runs were also made with the two acids in which the two phases were in distribution equilibrium so that there was adsorption but no transfer across the interface.

Table 1 lists the physical properties of interest for the solutes in solution. The equilibrium interfacial tensions were measured using the drop volume method with the correction factors of Harkins and Brown (*13*) and are shown in Figures 11 and 12. The interfacial tensions of both *n*- and isobutyric acids were found to be linear with concentration below an aqueous phase concentration of 0.01 molal. The concentration of solute in the aqueous phase in equilibrium with the oil phase was measured with a Bryce-Phoenix differential refractometer, and the distribution coefficient was determined by applying a mass balance.

RESULTS AND DISCUSSION

The surface pressure, $\pi = \sigma_{\text{pure}} - \sigma_{\text{with solute}}$, is related to the amount adsorbed in the linear adsorption region by $\pi = \Gamma RT$. Furthermore, a reduced surface pressure, $\pi_R(t) = \pi(t)/\pi_{x=x_0}$, is equivalent to the normalized amounts adsorbed, $\Gamma(t)/cx_0$ in the linear region. It is seen from Equations (11), (18), (23), and (25) that this normalized amount adsorbed is a function of time alone, independent of the initial concentration for a given system. Thus, on the average, the reduced surface pressure for a given solute and direction of transfer will have the same time behavior for any initial concentration within the linear adsorption region. A mean reduced surface pressure for a given time t may be calculated for a series of N runs by

$$\overline{\pi}_R(t) = \sum_{i=1}^{N} \pi_i(t) \Big/ \sum_{i=1}^{N} \pi_i, \quad x = x_0 \qquad (31)$$

This method of determining the mean is used rather than an arithmetic average of the individual reduced surface pressures so that the errors in the individual measurements of $\pi_i(t)$ are weighted equally. Figures 13, 14, 15, and 16 show the data for normal and isobutyric acids transferring from oil to water and from water to oil. The curves are from the analytical solutions.

It can be seen on both Figures 13 and 14 that the experimental surface pressure is always greater than that for the diffusion-controlled case. This indicates the presence of a net desorption barrier for transfer from oil to water for both acids. The data for transfer in the opposite direction, however, fall within experimental error of the no barrier curve. Unfortunately, because the mass distribution coefficient heavily favors the aqueous phase, the no barrier curve and that for even an infinitely large desorption barrier are indistinguishable by this experimental method. Though not shown here, the data for adsorption with no transfer across the interface are all within experimental error of the steady state values.

Regarding experimental error, it should be noted that the difference in diameter of two jets with different interfacial tensions is smallest near the nozzle. Therefore the interfacial tension determination near the nozzle was more sensitive to error in measurement of the diameter than it was farther downstream. A 0.01-in. error in the magnified diameter measurement could result in an error of as much

TABLE 1. PHYSICAL PROPERTIES OF SOLUTES IN SOLUTION, 23.5°C.

Solute	Diffusivities, sq. cm./sec. Water	Oil	Adsorption coefficient $= (\partial\Gamma/\partial x)$, cm.	Distribution coefficient m_w/m_0 (molalities)
n-Butyric acid	0.98×10^{-5}*	4.9×10^{-7}†	1.48×10^{-5}	$5\text{-}5m_w$
Isobutyric acid	0.95×10^{-5}*	4.9×10^{-7}†	1.48×10^{-5}	$11\text{-}57m_w$
1,5-Pentanediol	0.85×10^{-5}‡	4.6×10^{-7}†	?	Very large

* Reference 5.
† Estimated from Scheibel modification of Wilke-Chang equation.
‡ Wilke-Chang, (*38*).

as 2.4 dynes/cm. at a flow rate of 2.52 cc./sec. and as much as 4.3 dynes/cm. at a flow rate of 3.48 cc./sec. within 1 mm. of the nozzle, while that same error would result in interfacial tension errors of only 0.6 and 0.7 dynes/cm., respectively, 1 cm. downstream. Unfortunately, the first half-second of the interface age occurs within about 1 mm. of the nozzle. The effect of an inaccurately adjusted flow rate, however, is least near the nozzle, and greatest about 2 cm. downstream. A 1% error in flow rate results in an error in interfacial tension of from 0.2 to 0.4 dynes/cm. near the nozzle and 0.8 to 1.3 dynes/cm. 2 cm. downstream for the two flow rates, respectively.

The averaging of the data tends to smooth these errors, but it can be seen in Figures 13 through 16 that below an interface age of 0.5 sec. the scatter is still much worse than at greater ages. The data below 0.5 sec. were therefore ignored in the rate constant determinations. Desorption rate constants were estimated from the data to be on the order of 4 to 5 sec.$^{-1}$ for isobutyric acid and 5 to 10 sec.$^{-1}$ for *n*-butyric acid transferring from oil to water. The adsorption rate constants for transfer in the opposite direction are apparently greater than 100 sec.$^{-1}$. Since the proposed mechanisms for adsorption and desorption are reversible, knowledge of one of the rate constants enables estimation of the other, that is

$$K_{II} = k_2/k - 2 = \frac{\delta m}{c}$$

or

$$k_{-2} = k_2 \frac{c}{\delta m}$$

$c/m = 1.5 \times 10^{-5}$ cm. for both acids, and δ has been estimated to be 9.86 Å. for *n*-butyric acid and about 9.0 Å. for isobutyric acid. Thus the adsorption rate constants corresponding to the estimated desorption rate constants are on the order of 800 to 1,500 sec.$^{-1}$ for *n*-butyric acid and 700 to 800 sec.$^{-1}$ for isobutyric acid transferring from water to oil.

The transfer of 1,5-pentanediol was studied, although the concentrations used were well out of the linear adsorption region. The dynamic interfacial tension data for transfer in each direction are presented in Figure 17. The

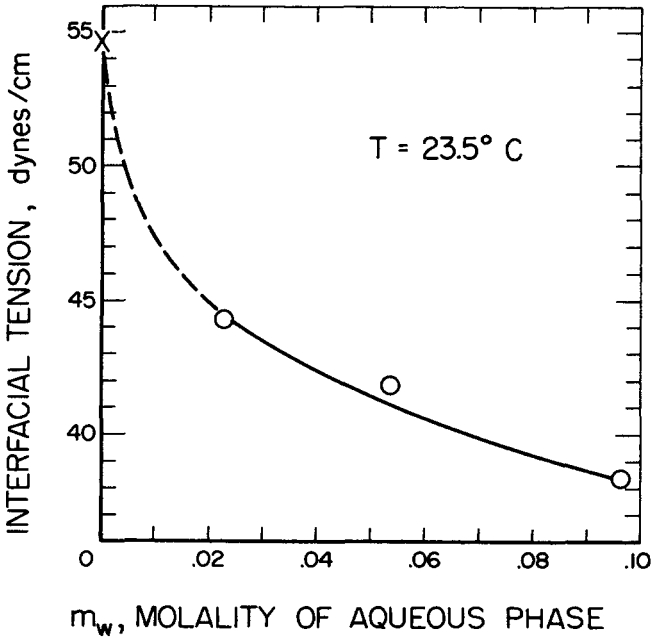

Fig. 12. Adsorption isotherm for 1,5-pentanediol at the water-Marcol 70 interface.

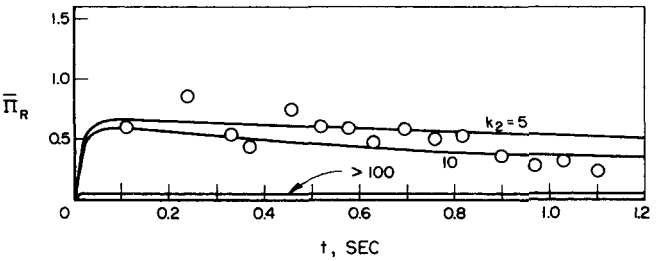

Fig. 13. Time dependence of surface pressure: *n*-butyric acid transferring from oil to water.

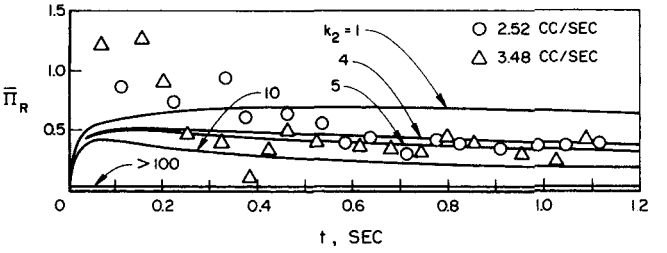

Fig. 14. Time dependence of surface pressure: isobutyric acid transferring from oil to water.

mass distribution coefficient for this solute is very large in favor of the aqueous phase, and for transfer from oil to water the interfacial tension should be near the pure liquid interfacial tension of 54.7 dynes/cm. However, the experimental interfacial tension continued to drop throughout the region of measurement. That the interfacial tension was much below the equilibrium value indicated the presence of a desorption barrier and that it dropped gradually indicated that an adsorption barrier must also have been present for transfer from oil to water. The data for transfer in the opposite direction also gave evidence of the presence of an adsorption barrier as the drop to the steady state value would have been almost instantaneous if there were no barrier. Because of the distribution coefficient heavily favoring the water phase the presence of a desorption barrier for transfer from water to oil could be detected by this method. The curves through the data in Figure 17 are drawn simply to show the trends.

CONCLUSIONS

1. Analytical solutions have been obtained for the transfer of an adsorbing solute across a liquid-liquid interface, taking into account the effects of molecular diffusion in both bulk phases, adsorptive accumulation at the interface, and energy barriers to adsorption and/or desorption. These solutions made possible the examination of the nature and relative importance of the above factors as they influence the mass transfer process. The calculations show that the effect of adsorptive accumulation alone on the overall mass transfer rate is small, generally yielding effective interfacial resistances of less than 10 sec./cm. for contact times in excess of 1 msec. On the other hand, adsorption and/or desorption barriers, depending on their magnitude, can produce large interfacial resistances persisting for long periods of time. Finally, the presence of a desorption barrier could cause the dynamic interfacial tension to pass through a minimum below the steady state value. Under the right conditions it may be possible for this dynamic interfacial tension to fall low enough so that a slight agitation could result in so-called spontaneous emulsification.

2. Dynamic interfacial tension data for oil-water systems with interface ages from 0.05 sec. to 1.5 sec. have been obtained using a laminar contracting liquid jet. The experimental data indicate the following:

There appears to be a net desorption barrier to the transfer of normal and isobutyric acids from Marcol-70 white

oil to water. The first-order desorption rate constants for these acids at room temperature are on the order of 5 to 10 sec.$^{-1}$ for *n*-butyric acid and 4 to 5 sec.$^{-1}$ for isobutyric acid.

There appear to be no adsorption barriers with rate constants smaller than 100 sec.$^{-1}$ to the transfer of these acids from water to oil. Any desorption barrier for transfer in this direction is undetectable by the present method for these particular systems because the distribution coefficient so heavily favors the aqueous phase.

There are apparently large barriers to both the adsorption and desorption of 1,5-pentanediol transferring from oil to water. A significant adsorption barrier is apparent for transfer in the opposite direction.

ACKNOWLEDGMENT

The authors acknowledge the financial assistance of the Office of Saline Water, U.S. Department of the Interior.

NOTATION

a = constants as defined in Equations (18) and (26)
b = constant as defined in Equations (18) and (26)
c = adsorption coefficient, $(\partial\Gamma/\partial x)_{x\to 0}$
d, e = constants as defined in Equation (26)
D = diffusivity
g = acceleration of gravity
h = vertical distance from jet nozzle
$k_1, k-2$ = rate constants for adsorption from phases 1 and 2, respectively
$k-1, k_2$ = rate constants for desorption from phases 1 and 2, respectively
K_I, K_{II} = interface-bulk equilibrium constants: $K_I = k_1/k-1$, $K_{II} = k_2/k-2$
m = distribution coefficient
Q = volumetric flow rate
r = jet radius
$r_{1,2,3}$ = roots as defined in Equation (26)
$R_{1,2}$ = principal radii of curvature of jet
R_i = interfacial resistance
t = time
u = linear velocity
W = combination of variables as defined in Equations (9) and (10)
x = solute concentration in phase 1
X = nondimensionalized solute concentration in phase 1

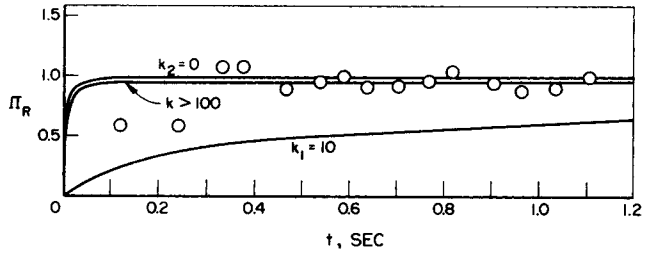

Fig. 15. Time dependence of surface pressure: *n*-butyric acid transferring from water to oil.

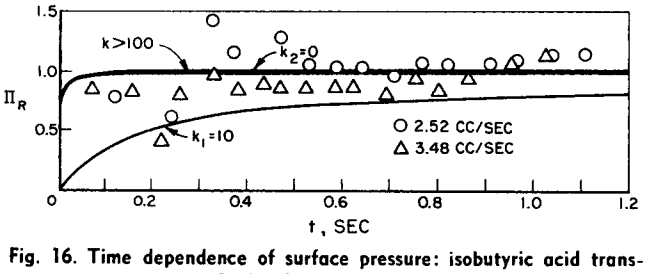

Fig. 16. Time dependence of surface pressure: isobutyric acid transferring from water to oil.

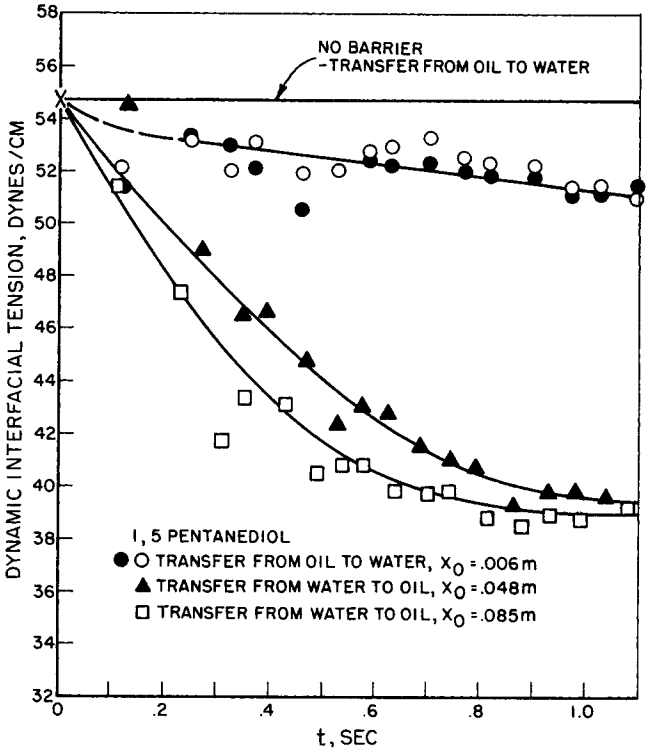

Fig. 17. Dynamic interfacial tension: 1,5-pentanediol transferring from oil to water and from water to oil.

y = solute concentration in phase 2
Y = nondimensionalized solute concentration in phase 2
z = distance measured from interface
α = coefficient of surface tension with solute concentration
β = constant as defined in Equations (9) to (11)
Γ = interfacial concentration
δ = interfacial layer thickness
ζ = dimensionless distance from interface, as defined in Equation (27)
η = constant as defined in Equation (23)
θ = dimensionless time, as defined in Equation (26)
κ = dimensionless rate constant, as defined in Equation (27)
π = surface pressure
ρ = density
σ = interfacial tension
σ_0 = interfacial tension in absence of solute
ϕ = parameter as defined in Equation (26)
ω = combination of variables as defined in Equation (11)
o = oil phase
w = aqueous phase
1 = phase 1
2 = phase 2

LITERATURE CITED

1. Addison, C. C., and T. A. Elliott, *J. Chem. Soc.*, 2789 (1949), 2090 (1950).
2. Baird, M. H. I., and J. F. Davidson, *Chem. Eng. Sci.*, **17**, 473 (1963).
3. Blokker, P. C., "Proceedings of the Second International Congress on Surface Activity," Vol. 1, p. 503, Academic Press, New York (1957).
4. Chiang, S. H., and H. L. Toor, *AIChE J.*, **5**, 165 (1959).
5. *Ibid.*, **6**, 539 (1960).
6. Cullen, E. J., and J. F. Davidson, *Trans. Faraday Soc.*, **53**, 113 (1957).

7. Davies, J. T., and J. B. Wiggill, *Proc. Roy. Soc. London*, **A255**, 277 (1960).
8. Duda, J. L., and J. S. Vrentas, *Chem. Eng. Sci.*, **22**, 27 (1967).
9. England, D. C., Ph.D. dissertation, Univ. Washington, Seattle (1968).
10. Garner, F. H., and P. Mina, *Trans. Faraday Soc.*, **55**, 1607 (1959).
11. *Ibid.*, **55**, 1617 (1959).
12. ———, and V. G. Jenson, *ibid.*, **55**, 1627 (1959).
13. Harkins, W. D., "The Physical Chemistry of Surface Films," p. 77, Reinhold, New York (1952).
14. Harvey, E. A., and W. Smith, *Chem. Eng. Sci.*, **10**, 274 (1959).
15. Hotta, H., and T. Isemura, *Bull. Chem. Soc. Japan*, **25**, 101 (1952).
16. Lewis, J. B., *Chem. Eng. Sci.*, **3**, 248 (1954).
17. *Ibid.*, **3**, 260 (1954).
18. MacNamey, W. J., *ibid.*, **15**, 210 (1961).
19. Nitsch, V. W., *Kolloid Z.*, **197** (1964).
20. ———, *Chem. Ing. Tech.*, **38**, 525 (1966).
21. Quinn, J. A., and P. G. Jeannin, *Chem. Eng. Sci.*, **15**, 243 (1961).
22. Raimondi, P., and H. L. Toor, *AIChE J.*, **5**, 86 (1959).
23. Scott, E. J., L. H. Tung, and H. G. Drickamer, *J. Chem. Phys.*, **19**, 1075 (1951).
24. Scriven, L. E., and R. L. Pigford, *AIChE J.*, **4**, 439 (1958).
25. Shain, S. A., and J. M. Prausnitz, *AIChE J.*, **10**, 766 (1964).
26. Shimbashi, T., and T. Shiba, *Bull. Chem. Soc. Japan*, **38**, 572 (1965).
27. *Ibid.*, **38**, 581 (1965).
28. Sinfelt, J. H., and H. G. Drickamer, *J. Chem. Phys.*, **23**, 1095 (1955).
29. Sutherland, K. L., *Australian J. Sci. Res.*, **A5**, 683 (1952).
30. Tung, L. H., and H. G. Drickamer, *J. Chem. Phys.*, **20**, 10 (1952).
31. Vignes, A., *J. Chim. Phys.*, **57**, 980 (1960).
32. Ward, A. F. H., "Surface Chemistry," p. 55, Butterworths, London (1949).
33. ———, and L. H. Brooks, *Trans. Faraday Soc.*, **48**, 1124 (1952).
34. Ward, A. F. H., and L. Tordai, *Nature*, **154**, 146 (1944).
35. ———, *J. Chem. Phys.*, **14**, 453 (1946).
36. ———, *Recueil Travaux Chim.*, **71**, 396, 482, 572 (1952).
37. Ward, W. J., and J. A. Quinn, *AIChE J.*, **11**, 1005 (1965).
38. Wilke, C. R., and P. Chang, *AIChE J.*, **1**, 264 (1955).

Manuscript received November 4, 1969; revision received February 23, 1970; paper accepted February 26, 1970.

Transient Flow in the Hydrodynamic Entrance Regions of Long Closed Ducts

CARL G. DOWNING

Oregon State University, Corvallis, Oregon

Velocity profiles were calculated for transient fluid flow in the hydrodynamic entrance regions of a long narrow slit and of a long tube. The solutions were obtained by use of a linearized momentum equation. An estimate was also made of the manner in which the resistance to flow of the entrance region develops with time.

The theoretical approach used by Sparrow, Lin, and Lundgren (2) in their analysis of steady flow in the entrance regions of closed ducts has been extended to the corresponding transient flow situation.

VELOCITY PROFILES

Consider the unsteady laminar incompressible flow of a Newtonian fluid in the entrance regions of (A) a tube and (B) a slit formed between two large parallel plates. The flow is described by the dimensional equations

$$\frac{\partial}{\partial x}(r^s u) + \frac{\partial}{\partial r}(r^s v) = 0 \qquad (1)$$

$$\frac{\partial u}{\partial t} + u\frac{\partial u}{\partial x} + v\frac{\partial u}{\partial r} = -\frac{1}{\rho}\frac{\partial P}{\partial x} + \nu\left\{\frac{\partial^2 u}{\partial x^2} + \frac{1}{r^s}\frac{\partial}{\partial r}\left(r^s\frac{\partial u}{\partial r}\right)\right\} \qquad (2)$$

where $s = 0$ and 1 for flow in a slit and in a tube, respectively. Taking the axial molecular transport of momentum to be negligible relative to the radial transport, and assuming that the pressure is constant across the section, one can linearize Equation (2):

$$\frac{\partial u}{\partial t} + \epsilon(x)\, U_\infty \frac{\partial u}{\partial x} = \Lambda(x,t) + \nu\frac{1}{r^s}\frac{\partial}{\partial r}\left(r^s\frac{\partial u}{\partial r}\right) \qquad (3)$$

where U_∞ is the average steady velocity and $\Lambda(x,t)$ includes the pressure gradient and residual inertia terms. The $\epsilon(x)$ are the same stretching parameters defined and evaluated by reference 2 and discussed by reference 3; they will not be further discussed here other than to note that $\epsilon(x)$ for a tube ranges from a value of 0.42 at $x = 0$ to an asymptotic value of 1.82 at large x, and that corresponding values for a slit are 0.37 and 1.135. Defining the following dimensionless variables

$$\omega = \frac{u}{U_\infty}, \quad \eta = \frac{r}{R}, \quad \tau = \frac{\nu t}{R^2}, \quad \text{and} \quad X^* = \frac{\nu x^*}{R^2 U_\infty}$$

where $dx = \epsilon(x)\, dx^*$, Equation (2) becomes

$$\frac{\partial \omega}{\partial \tau} + \frac{\partial \omega}{\partial X^*} = \Lambda^*(X^*,\tau) + \frac{1}{\eta^s}\frac{\partial}{\partial \eta}\left(\eta^s\frac{\partial \omega}{\partial \eta}\right) \qquad (4)$$

Integration of Equation (4) across the section yields

$$\left(\frac{1}{2^s}\right)\Lambda^*(X^*,\tau) = \frac{d}{d\tau}\int_0^1 \omega\,\eta^s\, d\eta - \left.\frac{\partial \omega}{\partial \eta}\right|_{\eta=1} \qquad (5)$$

which shows that $\Lambda^*(X^*,\tau)$ may be written as the sum of a macroscopic inertia term and a viscous friction term. Substitution of Equation (5) into Equation (4) then yields the following formulation of the problem:

$$\frac{\partial \omega}{\partial \tau} + \frac{\partial \omega}{\partial X^*} = (2^s)\frac{d}{d\tau}\int_0^1 \omega\,\eta^s\, d\eta$$

Carl G. Downing is now a consulting engineer in Corvallis, Oregon.